Journal of Sciences, Islamic Republic of Iran 17(1): 43-52 (2006) http://jsciences.ut.ac.ir
University of Tehran, ISSN 1016-1104

Synthesis, Characterization and Studies on Catalytic Behavior of Mn(Π) Complex with 2, 2′ Bipyridine, 1, 1′ Dioxide Ligand within Nanoreactors of MCM-41

R. Malakooti,[1] F. Farzaneh,[1,*] and M. Ghandi[2]

[1] *Department of Chemistry, University of Alzahra, Tehran, Islamic Republic of Iran*
[2] *School of Chemistry, University College of Science, University of Tehran, Tehran, Islamic Republic of Iran*

Abstract

Manganese (Π) complex with 2, 2′ bipyridine, 1, 1′ dioxide (bpdo) ligand was immobilized within nanoreactors of MCM-41. The immobilized complex was characterized by powder x-ray diffraction (XRD), nitrogen adsorption desorption, and FTIR. The pore volume, surface area and pore diameter of MCM-41 decreased after immobilization of Mn complex. Three bands observed at 1250, 1220 cm^{-1} and 757 cm^{-1} are attributed to the NO stretching and bending vibrations respectively. It was found that the immobilized Mn complex on MCM-41 successfully catalyzed the oxidation of cyclohexene, styrene, norbornene, and trans-stilbene with tert-butylhydroperoxide (TBHP).With the exception of cyclohexene, the other three olefins afforded the corresponding epoxides efficiently. Preparation and catalytic effect of Mn salt either on MCM-41 or modified MCM-41 with aminopropyltriethoxysilane; MCM-41(AP) will be discussed.

Keywords: MCM-41; Oxidation catalyst; Mn (II) complex; 2, 2′-Bipyridine, 1, 1′ dioxide ligand

Introduction

Mesostructured materials have certainly brought a new dimension to the design of catalysts. This potential is currently under intense study in a very large variety of catalytic applications such as hydrotreating, alkylation and polymerization [1].

The redox chemistry of Mn relies on the role of numerous metaloenzymes. In biological systems, Mn may be present as mono or dinuclear, or as a cluster of higher nuclearity. The mimicking of the structures and functions of theses enzymes has lead to inorganic synthesis of different Mn complexes with different bidentate ligands [2].

In past decade, much effort has been made on using of Mn complexes as homogeneous catalysts of oxidation reactions [3-13]. In order to heterogenize Mn complexes within solid supports, different media such as polymers [8,14-16], zeolites [17-29] and mesoporous silica have been investigated [30-40]. Some of these heterogeneous catalysis systems have been used for oxidation of diphenylmethane and trans-stilbene to benzophenone and trans-stilbene epoxide respectively. Recently, Mn-MCM-41 was also used as catalyst [41-55] for hydroxylation of benzene [42], oxidation of ethylbenzene to acetophenone [46] and oxidation of cyclohexene to cyclohexenol and cyclohexenone [47].

Unlike zeolites, the pore size of mesoporous silica is large enough to accommodate a variety of large molecules. Moreover, the high density of silanol groups

* *E-mail: faezeh_farzaneh@yahoo.com*

on the pore walls is beneficial for introducing a variety of functional groups. The surface modification has generally been achieved by post-grafting synthesis methods with organoalkysilanes. For this, surface-immobilized manganese complexes on amino-functionalized MCM-41 were synthesized and have been developed as epoxidation catalysts of styrene [56-59] and α- metlylstyrene [60-62].

In this study, Mn(Π) complex with oxygen donor ligand 2, 2′ bipyridine 1, 1′ dioxide (bpdo) was prepared and subsequently immobilized within nanoreactors of MCM-41 in order to study its catalytic effect in the oxidation of alkenes. Amino-functionalized MCM-41, MCM-41(AP) and $MnCl_2$/MCM-41(AP) were also prepared and studied in similar oxidation reactions.

2. Experimental

2.1. Materials

All chemicals were purchased from Merck Chemical Company and were used without further purification.

2.2. Instrumentation

Powder X-ray diffraction data were recorded by SIEFERT 3003 PTS diffractometer using a Cu K_α radiation. The FTIR spectra in the mid-IR region were obtained with KBr pellets using a Bruker FT-IR spectrometer (Tensor 27). The surface area, pore volume, pore size distribution and N_2 adsorption isotherms were determined using an ASAP 2000 (Micrometer) instrument. The oxidation products were separated and identified with Agilent 6890 series gas chromatograph equipped with a HP-5 capillary column (cross-linked 5%-phenyl methyl siloxane gum phase, 30.0 m × 530 μm × 1.50 μm nominal) and gas chromatograph-mass spectrometer (GC-MS; Agilent Technologies 6890 N network mass-selective detector) HP-5 HS capillary column (30 m × 0.250 mm × 0.25 μm).

2.3. Preparation of MCM-41

MCM-41 was prepared according to the procedure described previously [63]. The synthesis of MCM-41 was carried with the molar compositions of 1.00 SiO_2: 0.54 NaOH: 0.5 CTMABr (cetyltrimethylammonium bromide): 0.34 HCl: 100 H_2O.

2.4. Immobilization of $MnCl_2$ within Nanoreactors of MCM -41

One mmol of $MnCl_2.4H_2O$ in 5 ml of ethanol was slowly added to 1 g of MCM-41 in 5 ml of ethanol. The mixture was heated under reflux condition for 2 h. The solid product was then filtered and washed with hot ethanol. The Mn and Cl percentages were determined by AAS were 2.6% and 0.39%, respectively.

2.5. Synthesis of bpdo ligand

2, 2′-Bipyridine-1, 1′-dioxide (bpdo) was prepared according to the procedure described previously [64].

2.6. Synthesis of $Mn(bdpo)_2Cl_2$

This compound was prepared according to the procedure reported by Simpson and co-workers [64].

2.7. Immobilization of $Mn(bdpo)_2Cl_2$ within nanoreactors of MCM-41

0.2 g of $Mn(bdpo)_2Cl_2$ in 5 ml of ethanol was slowly added to 1 g of MCM-41 in 5 ml of ethanol. The resultant mixture was refluxed for 24 h under N_2. The mixture was then filtered and the solid was washed with ethanol. The AAS determination showed the percentage of Mn and Cl were 4.40 and 5.72, respectively.

2.8. Synthesis of MCM-41 (AP)

Functionalized MCM-41 or MCM-41(AP) was prepared according to the procedure described previously [65].

2.9. Immobilization of $MnCl_2$ within Nanoreactors of MCM-41

One mmol of $MnCl_2.4H_2O$ in 5 ml of ethanol was slowly added to 1 g of MCM-41(AP) in 5 ml of ethanol. The mixture was stirred under reflux condition for 2 h. The immobilized product was then filtered, washed with ethanol and dried at room temperature.

2.10. Oxidation of Olefins, General Procedure

Oxidation reactions were carried out in a stirring round bottom flask fitted with a water-cooled condenser and under atmospheric pressure in different solvents. Typically, 0.2 g of catalyst and 20 mmole of substrate in 6 ml of solvent were added into the reaction flask with slow stirring. After a few minutes, TBHP (24 mmole) was added, and the reaction mixture was refluxed for eight hours. After filtration, the solid was washed with solvent and the filtrate was subjected to GC analysis.

3. Results and Discussion

3.1. X-ray Diffraction Study

The low angle XRD patterns of calcined MCM-41, $MnCl_2$/MCM-41, MCM-41(AP), $MnCl_2$/MCM-41(AP) and $Mn(bpdo)_2Cl_2$/MCM-41 are shown in Figure 1. The calcined MCM-41 exhibits a very intense peak corresponding to 35A°d-spacing and three weak peaks at 21, 19 and 14 A°d-spacing (Fig. 1a). These four peaks can be indexed respectively as 100, 110, 200 and 210 reflections of the 2D hexagonal structure. These data are in good agreement with those reported before [66]. Figure 1b shows XRD pattern of $MnCl_2$/MCM-41 with a very intense peak corresponding to 37.58A°d-spacing and three other peaks. Similar results were obtained for $Mn(bpdo)_2Cl_2$/MCM-41. The intensity of $d_{(100)}$ decreased in the case of MCM-41(AP) and $MnCl_2$/MCM-41(AP).

3.2. Nitrogen Adsorption Measurements

The isotherms of nitrogen adsorption desorption of calcined MCM-41, $MnCl_2$/MCM-41, $Mn(bpdo)_2Cl_2$ /MCM-41, MCM-41(AP) and $MnCl_2$/MCM-41(AP) are shown in Figures 2 and 3, respectively. The BET surface area, unit cell, pore size and wall thickness are presented in Table 1. Three distinct well-defined stages in the isotherms were observed. The initial increase in nitrogen uptake at low p/p° may be due to monolayer absorption on the pore walls. A sharp step at p/p° ~0.3 indicates the capillary condensation in the mesopor. The plateau portion at high p/p° is associated with multilayer adsorption on the external surface of the catalyst. The mesoporous nature of the MCM-41, $MnCl_2$/MCM-41 and $Mn(bpdo)_2Cl_2$/MCM-41 materials shows a characteristic step at p/p°≈0.3 [46]. The sharpness and height of the capillary condensation step indicates the uniform distribution of pore size. Calculations using BJH method show that MCM-41 has a narrow pore size distribution with an average pore diameter of about 28A° (Figs. 4, 5). The measured surface area, pore diameter and wall thickness of the MCM-41 were in good agreement with reported results [67]. The p/p° position of the inflection point is a function of the pore diameter. A step rise in the range of 0.24-0.32 Pa is caused by the capillary condensation of nitrogen in the mesopor. This rise became more gentle and shifts to lower relative pressure in $Mn(bpdo)_2Cl_2$/MCM-41, MCM-41(AP), $MnCl_2$/MCM-41(AP). According to the results obtained, the BET surface area, pore size and wall thickness varied from 1212, 23 and 10.9 to 377, 24.5 and 17.51 A°, respectively. It was also observed that the hysteresis loops became smaller and the amount of N_2 adsorption decreases in MCM-41(AP), $MnCl_2$/MCM-41(AP) and $Mn(bpdo)_2Cl_2$/MCM-41. These results clearly indicate that immobilized Mn complex molecules prefer to initially locate within the MCM-41 nanoreators. Moreover, the very narrow hysteresis loop also indicates that the pore connectivity becomes facile and contains sharp capillary condensation and high systematic pore size distribution [33].

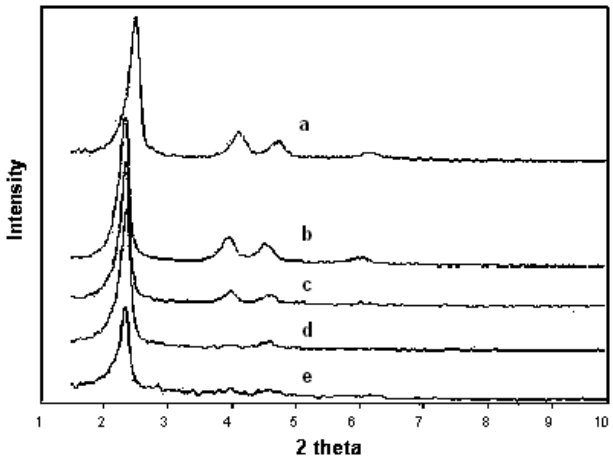

Figure 1. XRD of: (a) Calcined MCM-41, (b) $MnCl_2$/MCM-41 (2), (c) $Mn(bpdo)_2Cl_2$/ MCM-41 (3), (d) MCM-41(AP), (e) $MnCl_2$/MCM-41(AP).

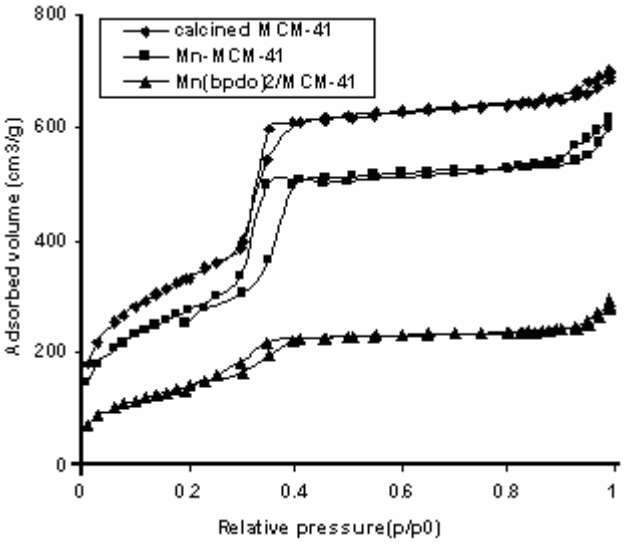

Figure 2. N_2 adsorption isotherm, Mn/MCM41 means $MnCl_2$/MCM-41.

3.3. FTIR Spectroscopy

The FTIR spectra of bpdo ligand, $Mn(bpdo)_2Cl_2$ complex and $Mn(bpdo)_2Cl_2$/MCM-41 are shown in Figure 6. The FT-IR spectrum of bpdo ligand shown in Figure 6a contains a band at 3250cm^{-1}, two bands at 1256, 1220 cm^{-1} and two bands around 845 cm^{-1} due to C-H (bipyridine oxide ring), NO stretchings and NO bending, respectively [64,69]. The FT-IR spectrum of $Mn(bpdo)_2Cl_2$ is shown in Figure 6b [64]. Compared to the uncomplexed ligand, the two NO stretching bands of bpdo has undergone a rather mark change due to coordination and appeared as an intense doublet. This result is similar to that reported previously [69].The two NO bending bands at 852-840 cm^{-1} also shifted to a lower frequency by the amount of 20 cm^{-1}. This indicates that the bpdo molecule either in the free solid or in the complex exists in gauche conformation. After immobilization of $Mn(bpdo)_2Cl_2$ complex within nano-oreactors of MCM-41 (Fig. 6c), two bands at 1252-1220 and 850 cm^{-1} were observed due to NO stretching and bending vibrations, respectively. Interestingly, although the N-O stretching and bending vibrations of complex appear in similar shape, they shift to a lower frequency with decreasing in band intensity. These results indicate that the complex is accommodated within the nanoreactors of MCM-41 in gauche conformation.

The IR spectra of MCM-41, $MnCl_2$/MCM-41, MCM-41(AP) and $MnCl_2$/MCM-41(AP) are shown in Figure 7. A broad band at ~3363-3280 cm^{-1} superimposed on MCM-41 broad hydroxyl band can be assigned to amino (asymmetric and symmetric stretchings) groups (Fig. 7a, b). A very weak and relatively broad band at ~1650 cm^{-1} can be assigned to amino deformation. The MCM-41(AP) broad band at region 3000-2800 cm^{-1} is observed which is due to -$(CH_3)_3$-NH_2 group. These observations clearly indicate that MCM-41 has been modified by 3-aminopropyltriethoxysilane (AP). After immobilization of $MnCl_2$ within MCM-41(AP), the average mid point of broad band at 3500 cm^{-1} shifts to a lower frequency with concomitant decreasing in intensity due to decrease of the number of OH groups in MCM-41(AP) (Fig. 7c, d).

To choose the proper solvent, the oxidation of norbornene with TBHP in the presence of $Mn(bpdo)_2Cl_2$/MCM-41 was carried out in dichloromethane, chloroform and acetonitrile for 6 h under reflux conditions. The results are shown in Table 2. It is evident that acetonitrile is the best medium since norbornene is oxidized selectively to the corresponding epoxide with the highest conversion percentage (90%). Therefore, other oxidation reactions were examined in this solvent with proper reaction time.

Cyclohexene was selected as the representative alkene in order to optimize the manganese mole numbers required per gram of solid support. The results are presented in Table 3. The oxidation results of norbornene, styrene, and trans-stilbene carried out under the most proper conditions of catalyst concentration per gram of solid supports and reaction times are shown in Table 4. We have included the effect of $MnCl_2$-MCM-41 in this Table in order to make the comparison with the effect of Mn complexes more convenient.

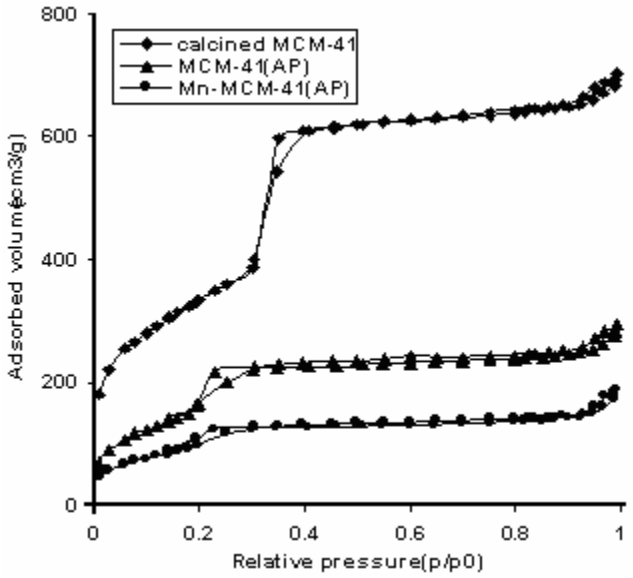

Figure 3. N_2 adsorption isotherm.

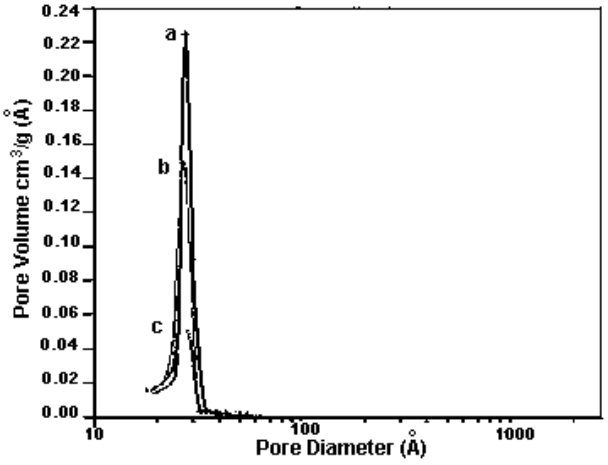

Figure 4. Pore size distribution of: (a) Calcined MCM-41, (b) $MnCl_2$/MCM-41(2), (c) $Mn(bpdo)_2Cl_2$/ MCM-41 (3).

Inspection of the results in Table 3 and observation of mixed peroxide (cyclohex-2-enyl) (tert-butyl) peroxide as the main product reveals that the radical pathway is dominant in this oxidation reaction. This conclusion has been driven from the worthy work of Sherington and his co-workers who believe that the formation of the mixed peroxide provides a rather strong evidence for the involvement of t-BuOO radical intermediate in reaction [70]. Therefore, Mn(Π) catalyzes free radical processes by promoting the decomposition of TBHP into chain initiating alkoxy and peroxy radicals in one electron transfer process [71] (Scheme 1). Due to lower selectivity of alkylperoxy radical in comparison to that of arylperoxy radical, hydrogen abstraction is dominant relative to addition to double bond [72]. As seen in Table 3, (cyclohex-2-enyl) (tert-butyl) peroxide is formed with the most selectivity in the presence of $Mn(bpdo)_2Cl_2$/MCM-41. Since electron transfer from TBHP to Mn(Ш) depends either on the electron deficiency of the complex ligands around the central cation or the basicity of the ligands (Scheme 1), this result is expected due to the highest electron demand of the manganese cation in this complex in comparison with other systems. The amount of (cyclohex-2-enyl) (tert-butyl) peroxide was previously shown to depend on the basicity strength of the ligands [70].

The results obtained from the oxidation of norbornene are shown in Table 4. Since hydrogen abstraction from this substrate leads to the formation of unstable bridgehead radical [72], addition of alkylperoxy radical to double bond and subsequent formation of the corresponding epoxide is the only route available for this olefin. We have observed the similar behavior under different catalysis systems [73].

The oxidation of styrene gave several products from which benzoic acid is dominant (Table 5). It seems likely to believe that benzaldehyde and benzoic acid have arisen from styrene epoxide as the preliminary oxidation product. This proposal is based on the recent publication by Hulea and his coworker who observed the similar results in the presence of Ti-containing molecular sieves as catalyst [74]. The implication of styrene peroxide and subsequent conversion to other products including benzaldehyde and benzonic acid was uncovered since using this epoxide as starting material under reaction conditions led to the formation of similar product mixture [74].

Oxidation of trans-stilbene with TBHP resulted in the formation of products as shown in Table 6. Interestingly, trans-stilbene epoxide is the dominant product under these reaction conditions. Compared to styrene oxidation, the stilbene epoxide is cleaved to benzaldehyde by a lesser extent. This is easily inferred since the presence of a phenyl group at each epoxide carbon sterically retards the approach of the TBHP molecule as attacking nucleophile. Takehira and his co-workers have shown that epoxidation of either cis or trans-stilbene with TBHP in the presence of manganese-containing MCM-41 leads mainly to the formation of trans- stilbene epoxide and benzaldehyde in similar product distributions [75]. The two isomers differ only in their conversion rates so that cis-stilbene was converted much lower than that of trans-stilbene due to the steric hinderance of phenyl groups that retards the

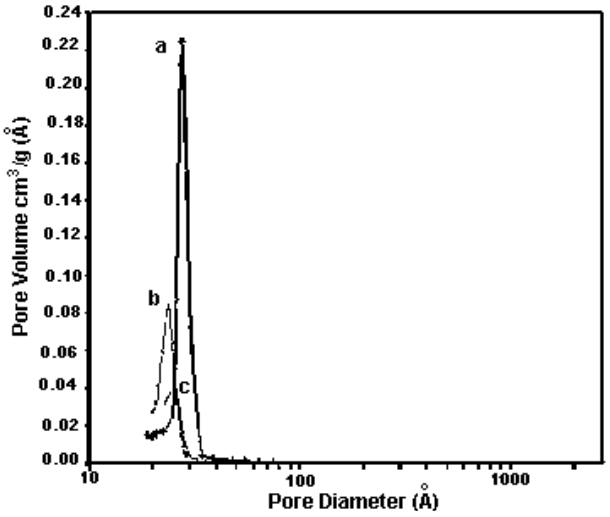

Figure 5. Pore size distribution of: (a) Calcined MCM-41, (b) MCM-41(AP) (c) $MnCl_2$/MCM-41(AP).

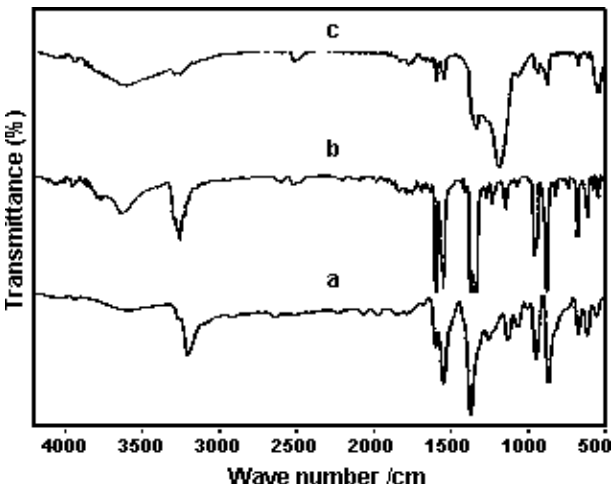

Figure 6. FT-IR spectra of: (a) bpdo ligand; (b) $Mn(bpdo)_2Cl_2$complex (c) $Mn(bpdo)_2Cl_2$/MCM-41.

Table 1. Physicochemical characterization of calcined MCM-41 and Mn catalysts

Sample	Calcined (Å)		BET surface area	Pore size	Wall thickness
	d-spacing value	Unit cell parameter	(m^2g^{-1})	(Å)	(Å)
MCM-41	35.14	40.62	1212	28	10.9
Mn/ MCM-41 (2)	37.58	43.44	1019	27.7	12.7
$Mn(bpdo)_2Cl_2$ / MCM-41 (3)	37.34	43.16	523	27	12.74
MCM-41(AP)	37.12	42.9	620	24.5	14.55
Mn/ MCM-41(AP) (2)	37.64	43.51	377	26	17.51

Unit cell parameter = $a_0 = 2d_{100}/\sqrt{3}$
Wall thickness = a_0-BJH pore diameter
Mn/MCM-41 and Mn/MCM-41(AP) mean $MnCl_2$/MCM-41 and $MnCl_2$/MCM-41(AP), respectively

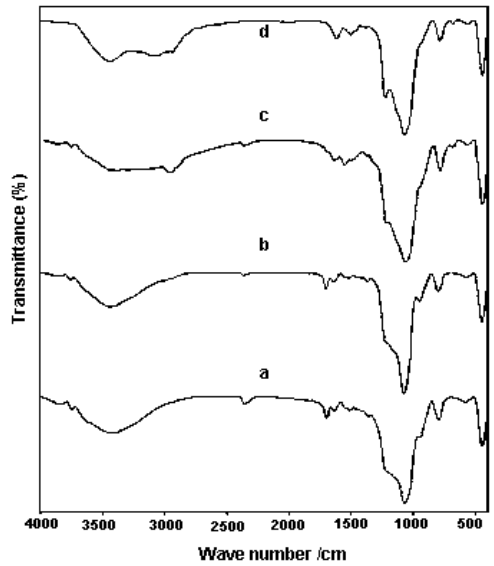

Figure 7. FT-IR spectra of: (a) Calcined MCM-41; (b) $MnCl_2$/MCM-41; (c) MCM-41(AP); (d) $MnCl_2$/MCM-41(AP).

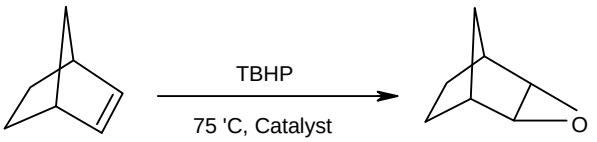

Table 2. Oxidation of norbornene with TBHP by $Mn(bpdo)_2Cl_2$/MCM-41 in various solvents

Run	Solvent	Conversion (%)	Epoxide selectivity (%)
1	CH_2Cl_2	45	100
2	$CHCl_3$	75	100
3	CH_3CN	87	100

Reaction condition: 0.2 g catalyst, 20 mmole substrate, 24 mmole TBHP, 3 ml solvent, Time: 6 h

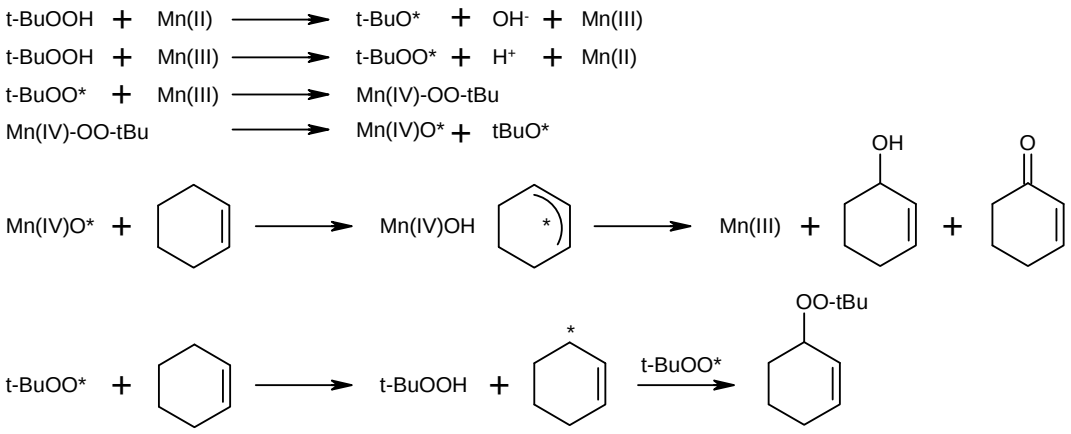

Scheme 1

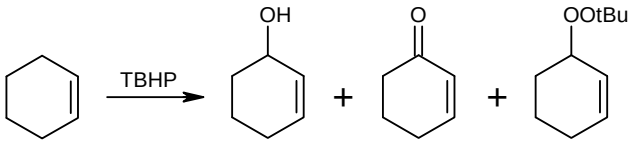

Table 3. Oxidation of cyclohexene with TBHP in the presence of Mn catalysts in CH3CN

Catalyst	Conversion (%)	Yield (%)		
		ol	*one*	*Cyclohexene-OOtBu*
Mn/MCM-41 (1)	47	34	10	56
Mn/MCM-41 (2)	60	29	30	41
Mn/MCM-41 (3)	48	20	34	46
$Mn(bpdo)_2Cl_2$/MCM-41 (1)	69	19		81
$Mn(bpdo)_2Cl_2$/MCM-41 (2)	49	27	1	72
$Mn(bpdo)_2Cl_2$/MCM-41 (3)	92	37	1	62
Mn/MCM-41 (AP) (1)	58	30	3	67
Mn/MCM-41 (AP) (2)	92	53		47
Mn/MCM-41 (AP) (3)	68	34		60

Reaction condition: 0.2 g catalyst, 20 mmole substrate, 24 mmole TBHP, 3 ml acetonitrile, Time: 8 h
(1): 0.0005 mole Mn in 1 g catalyst, (2): 0.001 mole Mn in 1 g catalyst, (3): 0.0015 mole Mn in 1 g catalyst

Table 4. Epoxidation of norbornene with TBHP by Mn catalysts

Catalyst	Conversion (%)	Epoxide selectivity (%)	Mn(%)	TON[a]
Mn/MCM-41 (2)	78	100	0.48	89655
$Mn(bpdo)_2Cl_2$/MCM-41 (3)	91	100	4.22	11895
Mn/MCM-41(AP) (2)	82	100	4.61	9820

Reaction condition: 0.2 g catalyst, 20 mmole substrate, 24 mmole TBHP, 3 ml acetonitrile, time reaction: 8 h
a: mmole products per mmole Mn

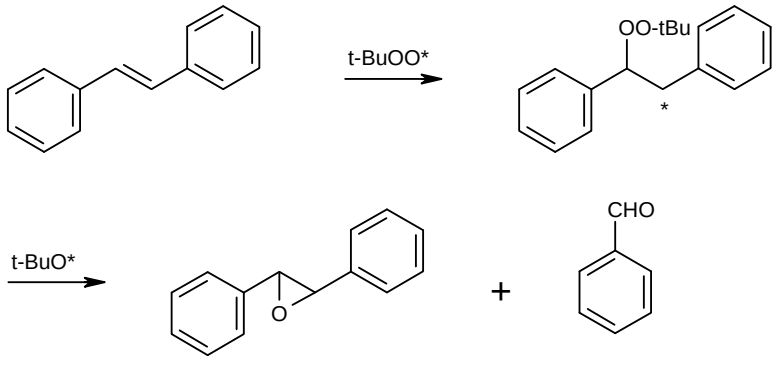

Scheme 2

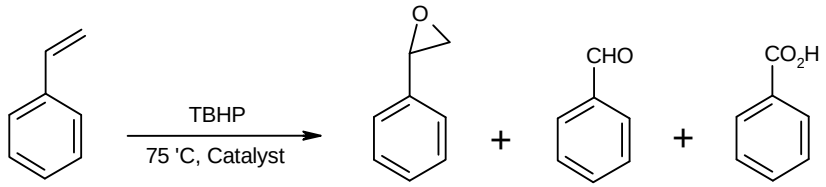

Table 5. Oxidation of styrene with TBHP by Mn catalysts

Catalyst	Conversion (%)	Selectivity (%)				Mn (%)	TON[a]
		Epoxide	*Benzaldehyde*	*Benzoic acid*	*Others*		
Mn/ MCM-41 (2)	41	4	8	70	18	0.48	47126
$Mn(bpdo)_2Cl_2$ / MCM-41 (3)	92	3	11	76	10	4.22	12026
Mn/ MCM-41(AP) (2)	60		15	84	1	4.61	7185

Reaction condition: 0.2 g catalyst, 20 mmole substrate, 24 mmole TBHP, 3 ml acetonitrile, time reaction: 12 h
a: mmole products per mmole Mn

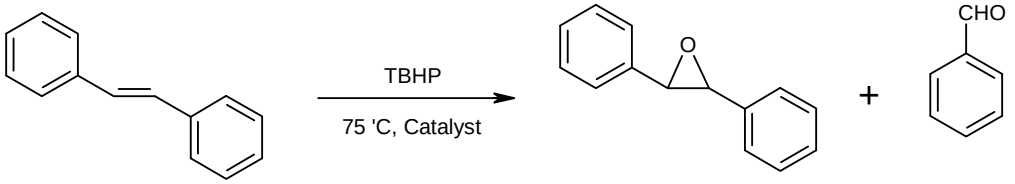

Table 6. Oxidation of Trans-Stilbene with TBHP by Mn Catalysts

Catalyst	Conversion (%)	Selectivity (%)			Mn (%)	TON[a]
		Epoxide	*Benzadlehyde*	*Others*		
Mn/MCM-41 (2)	90	49	2	50	0.48	5172
$Mn(bpdo)_2Cl_2$/MCM-41	75	60	20	20	4.22	490
Mn/MCM-41 (AP)	95	55	26	19	4.61	593
$Mn(bpdo)_2Cl_2$/Al-MCM-41	95	65	0	35	5.63	475

Reaction Condition: 0.2 g Catalyst, 1 mmole substrate, 10 mmole TBHP, DMF: CH3CN (1:4) 10 ml, time reaction: 12 h
a: mmole products per mmole Mn

reaction between substrate and oxygen species [75]. They believe that the oxidation reactions proceed through a radical intermediate. As soon as the double bond is cleaved as tBuOO radical is added, rotation around the single bond occurs and phenyl groups occupy the trans positions. Elimination of tBuO radical and subsequent formation of epoxy ring will finally yield the trans-stilbene epoxide (Scheme 2). On this basis, the exclusive formation of trans- stilbene epoxide from trans-stilbene finds support.

Conclusion

In this study, it was found that XRD patterns of $Mn(bdpo)_2$ Cl_2, and $MnCl_2$ within nanoreactors of MCM-41 show three low angle diffraction peaks, characteristic of mesoporous materials with hexagonal channels array and ordered pore systems. The higher unit cell parameter a_0 compared with pure MCM-41 silica is an indication of the presence of Mn complex and $MnCl_2$ within MCM-41 nanoreactors.

It was also found that $Mn(bdpo)_2Cl_2$/MCM-41 with clean and inexpensive TBHP is a remarkable combination for epoxidation of alkenes either without active allylic hydrogens or containing substitutions at either olefinic carbons. Since MCM-41 provides mesoporous pores to the guest molecules, our system is recommended for epoxidation of large alkenes.

Acknowledgement

The authors gratefully acknowledge University of Alzahra for financial support.

Reference

1. Sen S.E., Smith S.M., and Sullivan K.A. *Tetrahedron*, **55**: 12657 (1999).
2. De Vos D.E. and Jacobs P.A. *J. Mol. Catal. A: Chem.*, **117**: 57 (1997).
3. Jorgensen K.A. *Chem. Rev.*, **89**: 431(1989).
4. Corma A. *Ibid.*, **97**: 2373 (1997).
5. Zhang W., Loebach J.L., Wilson S.R., and Jacobsen E.N. *J. Am. Chem. Soc.*, **112**: 2801 (1990).
6. Zhang W. and Jacobsen E.N. *J. Org. Chem.*, **56**: 2296 (1991).
7. De Vos D.E. and Bein T. *J. Organometal. Chem.*, **520**: 195(1996).
8. Vankelecom F.J., Tas D., Parton R.F., Van de Vyver V., and Jacobs P.A. *Angew. Chem. Int. Ed. Engl.*, **35**(12): 1346 (1996).
9. De Vos D.E., Sels B.F., Reynaers M., Subba Rao Y.V., and Jacobs P.A. *Tetrahedron Lett.*, **39**: 3221 (1998).
10. Shimanovich R., Hannah S., Lynch V., Gerasimchuk N., Mody T.D., Magda D., Sessler J., and Groves J.T. *J. Am. Chem. Soc.*, **123**: 3613 (2001).
11. Van Gorkum R., Bouwman E., and Reedijk J. *Inorg. Chem.*, **43**: 2456 (2004).
12. Adam W., Humpf H.-U., Roschman K.J., and Saha-Moller C.R. *J. Org. Chem.*, **66**: 5796 (2001).
13. Cavallo L. and Jacobson H. *Ibid.*, **68**: 62 (2003).
14. Bein T. *Solid Catalysts and Porous Solids*. 85 (1999).
15. Minutolo F., Pini D., and Salvadori P. *Tetrahedron Lett.*, **37**(19): 3375 (1996).
16. Minutolo F., Pini D., Petri A., and Salvadori P. *Tetrahedron Asymmetry*, **7,8**: 2293 (1996).
17. Knops-Gerrits P.P. and DeVos D.E., Thibault-Starzyk F., and Jacobs P.A. *Nature*, **396**: 543 (1994).
18. DeVos D.E., Meinershagen L., and Bein T. *Angew. Chem. Int. Ed. Engl.*, **35**(19): 2211 (1996).
19. Sabater M.J., Corma A., Domenech A., Fornes V., and Garcia H. *Chem. Commun.*, **14**: 1285 (1997).
20. Ogunwumi S.B., Steven B., and Bein T. *Ibid.*, **9**: 901 (1997).
21. Farzaneh F., Soleimannejad J., and Ghandi M. *J. Mol. Catal. A*, **118**: 223 (1997).
22. Knops-Gerrits P.P., De Vos D.E., and Jacobs P.A. *Ibid.*, **117**: 57 (1997).
23. Jacob C.R., Varkey S.P., and Ratnasamy P. *Appl. Catal. A*, **182**: 91 (1999).
24. Salavati Niassary M., Farzaneh F., Ghandi M., and Turkian L. *J. Mol. Catal. A*, **157**: 183 (2000).
25. Wang R.M., Feng H.-X., He Y.-F., Xia C.-G., Suo J.-S., and Wang Y.-P. *Ibid.*, **151**: 253 (2000).
26. Sinha A.K., Satyanarayana C.V.V., Srinivas A.K.D., Sivasanker S., and Ratnasamy P. *Micropor. Mesopor. Mater.*, **35-36**: 471 (2000).
27. Diaz E., Ordonez S., Vega A., and Coca J. *J. Chromatogr. A*, **1049**: 161 (2004).
28. Poltowicz J. and Haber J. *J. Mol. Catal. A*, **220**: 43 (2004).
29. Martinez-Lorente M.A., Battioni P., Kleemiss W., Bartoli J.F., and Mansuy D. *Ibid.*, **113**: 343 (1996).
30. Luan Z., Xu J., and Kevan L. *Chem. Mater.*, **10**: 3699 (1998).
31. Eswaramoorthy M., Neeraj C.N., and Rao R. *Chem. Commun.*, 615 (1998).
32. Poltowicz J., Serwicka E.M., Bastardo-Gonzalez E., Jones W., and Mokaya R. *Appl. Catal. A*, **218**: 211 (2001).
33. Clemente-Leon M., Coronado E., Forment-Aliaga A., Martinez-Agudo J.M., and Amoros P. *Polyhedron*, **22**: 2395 (2003).
34. Gleizes A.N., Fernandes A., and Dexpert-Ghys J. *Journal of Alloys and Compounds*, **374**: 303 (2004).
35. Piaggio P., McMorn P., Murphy D., Bethell D., Bulman Page P.C., Hancock F.E., Sly C., Kerton O.J., and Hutchings G.J. *J. Chem. Soc. Perkin Trans.*, **2**: 2008 (2000).
36. Piaggio P., Langham C., McMorn P., Bethell D., Bulman-page P.C., Hancock F.E., Sly C., and Hutchings G.J. *Ibid.*, **2**: 143 (2000).
37. Caps V. and Tsang S.C. *Catal. Today*, **61**: 19 (2000).
38. Gnatyuk I., Gavrilko T., Puchkovska G., Chashechnikova I., Baran J., and Ratajczak H. *J. Mol. Struct.*, **614**: 233 (2002).
39. Li Z., Xia C.-G., and Zhang X.-M. *J. Mol. Catal. A*, **185**: 47 (2002).
40. Gleeson D., Burch R., Cruise N.A., and Tsang S.C. *Nanostructured Materials*, **12**: 1007 (1999).
41. Zhao D. and Goldfarb D. *J. Chem. Soc. Chem. Commun.*, 875 (1995).
42. Zhang W., Wang J., Tanev P.T., and Pinnovaia T. *J. Chem. Commun.*, 979 (1996).
43. Wang L-Z., Shi J.-I., Yu J., and Yan D.-S. *Nanostructured Materials*, **10,8**: 1289 **(**1998).
44. Burch R., Cruise N.A., Gleeson D., and Tsang S.C. *J. Mater. Chem.* **8,1**: 227 (1998).
45. Zhang J. and Goldfarb D. *Micropor. Mesopor. Mater.*, **48**: 143 (2001).
46. Vetrivel S. and Pandurangan A. *Appl. Catal. A*, **264**: 243 (2004).
47. Armbruster U., Martin A., Smejkal Q., and Kosslick H. *Ibid.*, **265**: 237 (2004).
48. Vetrivel S. and Pandurangan A. *J. Mol. Catal. A*, **217**: 165(2004).
49. Parvulescu V., Anastasescu C., and Su B.L. *Ibid.*, **211**: 143 (2004).
50. Xu J., Luan Z., Wasowicz T., and Kevan L., *Micropor. Mesopor. Mater.*, **22**: 179 (1998).
51. Yuan Z.-Y., Ma H.-T., Luo Q., and Zhou W., *Materials Chemistry and Physics*, **77**: 299 (2002).
52. Selvarj M., Sinha P.K., Lee K., Ahn I., Pandurangan A., and Lee T.G. *Micropor. Mesopor. Mater.*, **78**: 139 (2005).
53. Zhang Q., Wang Y., Itsuki S., Shishido T., and Takehira K. *J. Mol. Catal. A*, **188**: 189 (2002).
54. Aronson B.J., Blanford C.F., and Stein A. *J. Phys. Chem. B*, **104**: 449 (2000).
55. Vetrivel S. and Pandurangan A. *J. Mol. Catal. A*, **227**: 269 (2005).
56. Sutra P. and Brunel D. *Chem. Commun.*, 2485 (1996).

57. Subba Rao Y.V., De Vos D.E., Bein T., and Jacobs P.A. *Ibid.*, 355 (1997).
58. Chisem J., Chisem I.C., Rafelt J.S., Macquarrie D.J., and Clark J.H. *Ibid.*, 2203 (1997).
59. Brunel D. *Micropor. Mesopor. Mater.*, **27**: 329 (1999).
60. Joong Kim G. and Hoon Shin J. *Tetrahedron Lett.*, **40**: 6827 (1999).
61. Xiang S., Zhang Y., Xin Q., and Li C. *Chem. Commun.*, (2002) 2696.
62. Bigi F., Moroni L., Maggi R., and Sartori G. *Ibid.*, 716 (2002).
63. Feaston B.P. and Higgins J.B. *J. Phys. Chem.*, **98**: 4459 (1994).
64. Simpson P.G., Vinciguerra A., and Quagliano J.V. *Inorg. Chem.*, **2,2**: 282 (1963).
65. Kanno H., Yamamoto J., Murahashi S., Utsuno S., and Fujita J. *Bull. Chem. Soc. Jpn.*, **64**: 2936 (1991).
66. Zheng S., Gao L., and Guo J. *J. Solid State Chem.*, **152**: 447 (2000).
67. Zhao X.S., Lu G.Q., and Hu X. *Micropor and Mesopor. Mat.*, **41**: 37 (2000).
68. Lyneh J. *Physico-Chemical Analysis of Industrian Catalysis*. Edition Technip Paris, pp. 7-18 (2001).
69. Vinciguerra A., Simpson P.G., Kakiuti Y., and Quagliano J.V. *Inorg. Chem.*, **2,2**: 286 (1963).
70. Olason G. and Sherrington D.C. *Reactive & Functional Polymers*, **42**: 163 (1999).
71. Arends I.W.C.E. and Sheldon R.A. *Appl. Catal. A*, **22**: 175 (2001).
72. March J. *Advanced Organic Chemistry*. Third Edition, John Wiley & Sons, New York, p. 616 (1985).
73. Ghadiri M., Farzaneh F.,.Ghandi M., and Alizadeh M., *J. Mol. Catal. A*, **233**: 127(2005).
74. Hulea V. and Dumitriu E. *Appl. Catal.*, **277**: 99 (2004).
75. Zhang Q., Wang Y., Itsuki S., Shishido T., and Takehira K. *J. Mol. Catal. A*, **188**: 189. (2002).